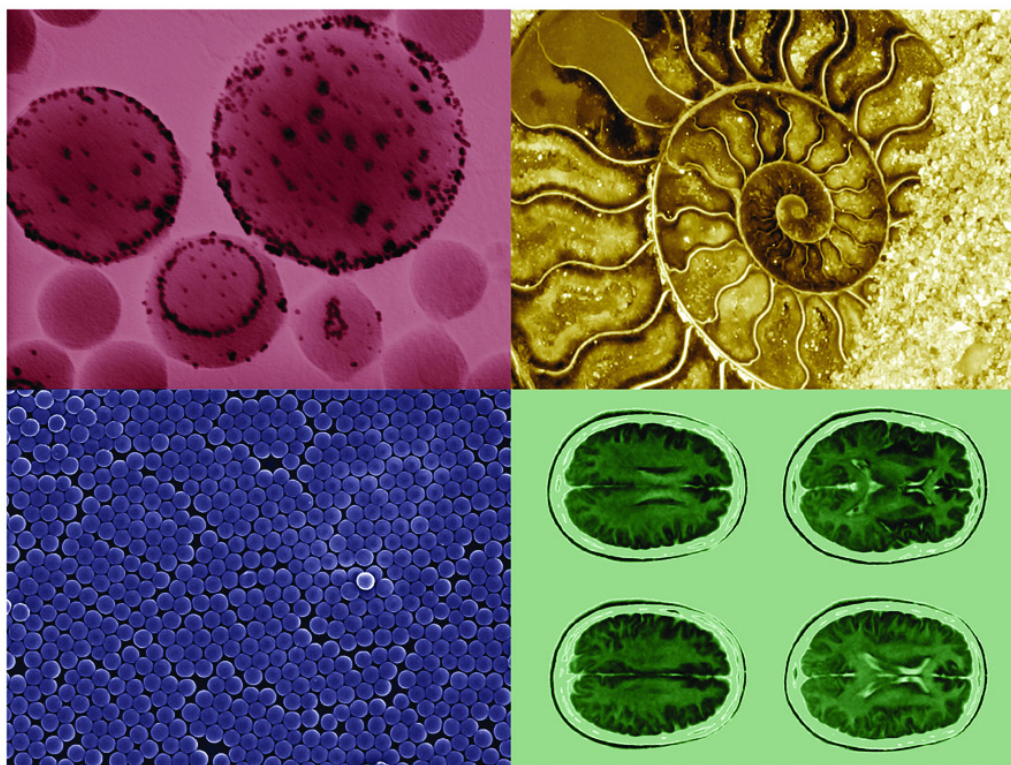


edited by Tito Trindade | Ana L Daniel da Silva

Nanocomposite Particles for Bio-Applications

Materials and Bio-Interfaces



Nanocomposite Particles for Bio-Applications

Materials and Bio-Interfaces

edited by Tito Trindade | Ana L Daniel da Silva

Nanocomposite Particles for Bio-Applications

Materials and Bio-Interfaces

Published by

Pan Stanford Publishing Pte. Ltd.
Penthouse Level, Suntec Tower 3
8 Temasek Boulevard
Singapore 038988

Email: editorial@panstanford.com

Web: www.panstanford.com

British Library Cataloguing-in-Publication Data

A catalogue record for this book is available from the British Library.

NANOCOMPOSITE PARTICLES FOR BIO-APPLICATIONS

Copyright © 2011 by Pan Stanford Publishing Pte. Ltd.

All rights reserved. This book, or parts thereof, may not be reproduced in any form or by any means, electronic or mechanical, including photocopying, recording or any information storage and retrieval system now known or to be invented, without written permission from the publisher.

For photocopying of material in this volume, please pay a copying fee through the Copyright Clearance Center, Inc., 222 Rosewood Drive, Danvers, MA 01923, USA. In this case permission to photocopy is not required from the publisher.

ISBN 978-981-4267-78-6 (Hardcover)

ISBN 978-981-4267-81-6 (eBook)

Printed in the USA

Contents

<i>List of Figures</i>	xi
<i>List of Tables</i>	xix
<i>Preface</i>	xxi
1. From Nanoparticles to Nanocomposites: A Brief Overview	1
1.1 Nanoscience and Nanotechnology: An introduction	1
1.2 Nanoparticles' Diversity	3
1.2.1 Quantum dots	4
1.2.2 Iron oxides	4
1.2.3 Metal nanoparticles	5
1.3 Surface Modification of Nanoparticles	7
1.3.1 Ligand exchange reactions	8
1.3.2 Inorganic nanocoating	8
1.3.3 Encapsulation in polymers	10
1.4 Designing Biointerfaces over Nanoparticles	11
1.5 Challenges for the Future... Nanosafety for Today	14
2. Polymers for Biomedical Applications: Chemical Modification and Biofunctionalization	21
2.1 Drug Delivery Systems	21
2.2 Hydrogels	23
2.2.1 Application of hydrogels	24
2.2.2 Types of hydrogels	25
2.3 Bioadhesives	30
2.4 Surface Modification	34
2.4.1 Surface modification by ultra-violet radiation	36
2.4.2 Plasma treatment	37
2.4.2.1 Plasma generation	37

2.4.2.2	Plasma polymerization and surface modification of polymers	38
2.5	Concluding Remarks	39
3.	Nanocapsules as Carriers for the Transport and Targeted Delivery of Bioactive Molecules	45
3.1	Introduction	45
3.2	Polymeric Nanocapsules: Production and Characterization	45
3.2.1	Nanocapsules made of synthetic polymers	47
3.2.1.1	Polyacrylate nanocapsules	47
3.2.1.2	Polyester nanocapsules	49
3.2.2	Nanocapsules made of natural polymers	50
3.2.3	Lipid nanocapsules	51
3.3	Therapeutical Applications of Nanocapsules	52
3.3.1	Nanocapsules for oral drug delivery	52
3.3.1.1	Nanocapsules for oral peptide delivery	52
3.3.1.2	Nanocapsules for oral delivery of lipophilic low molecular weight drugs	54
3.3.2	Nanocapsules as nasal drug carriers	55
3.3.3	Nanocapsules as ocular drug carriers	56
3.3.4	Nanocapsules in cancer therapy	58
3.3.5	Nanocapsules as carriers for gene therapy	59
3.4	Conclusions	60
4.	Inorganic Nanoparticles Biofunctionalization	69
4.1	Bioconjugation of Nanoparticles	69
4.2	Nanoparticles and Their Surface Properties	70
4.2.1	Surface capping of nanoparticles	70
4.2.2	Semiconductor quantum dots and metallic nanoparticles	71
4.2.3	Silica nanoparticles and silica encapsulation	72
4.3	Attachment Schemes	74
4.3.1	Covalent attachment	74
4.3.2	Non-covalent attachment	75
4.3.3	Affinity binding	76
4.4	Specific Cases	76
4.4.1	Proteins	76
4.4.2	DNA	78
4.4.3	Avidin	79
4.4.4	Phospholipid encapsulation and functionalization	81
4.5	Applications	83
4.5.1	Cellular imaging	83
4.5.2	Drug delivery	84

4.5.3	Bioluminescence resonance energy transfer	86
4.5.4	Hyperthermia	87
4.6	Conclusion	88
5.	Silica-Based Materials: Bioprocesses and Nanocomposites	97
5.1	Natural Silica Nanocomposites	97
5.1.1	Introduction	97
5.1.2	Diatom biosilica	98
5.1.3	Sponge biosilica	99
5.1.4	(Bio)-technological applications of biosilica	100
5.2	Biomimetic Silica Nanocomposites	102
5.2.1	Introduction	102
5.2.2	Silica nanocomposites based on natural templates	102
5.2.3	Silica nanocomposites based on model templates	103
5.2.3.1	Synthetic peptides	103
5.2.3.2	Synthetic polyamines	103
5.2.3.3	Biological templates	105
5.2.4	Biomimetism: How far can we go?	106
5.3	Bio-Inspired Silica Nanocomposites	107
5.3.1	Introduction	107
5.3.2	Biotechnological and medical applications	107
5.3.3	Perspectives	109
6.	Synthetic Strategies for Polymer-Based Nanocomposite Particles	115
6.1	Introduction	115
6.2	Surfaces and Interfaces: Chemical Modification of Nanoparticles	117
6.3	<i>In situ</i> Synthetic Strategies for Polymer-Based Colloidal Nanocomposites	120
6.3.1	<i>In situ</i> preparation of the fillers	121
6.3.1.1	Sol-gel methods	121
6.3.2	<i>In situ</i> polymerization of the matrix	123
6.3.2.1	Organic solvent-based methods: Dispersion polymerization	124
6.3.2.2	Water-based methods: Emulsion and miniemulsion polymerization	125
6.3.3	Controlled polymerization: Surface initiated polymerization (SIP)	128
6.3.3.1	Atom Transfer Radical Polymerization—ATRP	128
6.3.3.2	Reversible Addition Fragmentation chain transfer (RAFT) polymerization	130
6.3.3.3	Combined controlled polymerization mechanisms	132

6.4	Functionalization of Polymer-Based Nanocomposites for Bio-Applications	132
6.5	Final Remarks	134
7.	Synthesis of Nanocomposite Particles Using Supercritical Fluids: A Bridge with Bio-applications	145
7.1	Introduction	145
7.2	Supercritical Fluids: Definition and Current use in Bio-Applications	146
7.2.1	Definition	146
7.2.2	SCFs in biomedical applications	148
7.2.2.1	Development of drug delivery systems	148
7.2.2.2	scCO ₂ for purification and sterilization	150
7.3	Can SCFs be Used to Introduce Inorganic NPs into Polymers?	150
7.3.1	Formation of hybrid organic-inorganic NPs in SCFs (route 1)	152
7.3.2	Encapsulation of inorganic NPs into a polymer shell (route 2)	153
7.3.3	Polymer swelling and in situ growth of inorganic NPs (route 3)	154
7.3.3.1	Polymer swelling by scCO ₂	155
7.3.3.2	Chemical transformation of impregnated metal precursor	155
7.4	Conclusions	157
8.	Biocomposites Containing Magnetic Nanoparticles	165
8.1	Introduction	165
8.2	Magnetic Properties	167
8.2.1	Magnetism at nanoscale level: Concepts and main phenomena	167
8.2.1.1	Basic concepts	167
8.2.1.2	Systems with interactions between magnetic centers	168
8.2.1.3	Superparamagnetism	169
8.2.2	Magnetism concepts subjacent to bio-applications	172
8.2.2.1	Magnetic separation and drug delivery	172
8.2.2.2	Magnetic resonance imaging (MRI)	172
8.2.2.3	Magnetic hyperthermia	173
8.3	Magnetic Nanoparticles for Bio-Applications	175
8.3.1	Iron oxide nanoparticles	175
8.3.2	Metallic nanoparticles	176
8.3.3	Metal alloy nanoparticles	177
8.3.4	Bimagnetic nanoparticles	177

8.4	Strategies of Synthesis of Magnetic Biocomposite Nanoparticles . .	178
8.4.1	<i>In situ</i> formation of magnetic nanoparticles	179
8.4.1.1	Iron oxide nanoparticles	180
8.4.1.2	Other magnetic nanoparticles	183
8.4.2	Encapsulation of magnetic nanoparticles within biopolymers	185
8.5	Conclusions and Future Outlook	186
9.	Multifunctional Nanocomposite Particles for Biomedical Applications	193
9.1	Introduction	193
9.2	Types of Multifunctional Magnetic-Fluorescent Nanocomposites . .	194
9.3	Main Approaches to the Preparation of Multifunctional Magnetic-Fluorescent Nanocomposites	195
9.3.1	Silica coated magnetic-fluorescent nanoparticles	196
9.3.2	Organic polymer coated magnetic cores treated with fluorescent entities	198
9.3.3	Ionic assemblies of magnetic cores and fluorescent entities .	199
9.3.4	Fluorescently-labeled lipid coated magnetic nanoparticles .	200
9.3.5	Magnetic core directly linked to fluorescent entity via a molecular spacer	201
9.3.6	Magnetic cores coated by fluorescent semiconducting shells	201
9.3.7	Magnetically-doped QDs	202
9.3.8	Magnetic nanoparticles and QDs embedded within a polymer or silica matrix	203
9.4	Biomedical Applications	204
9.4.1	Bio-imaging probes	204
9.4.2	Cell tracking, sorting and bioseparation	206
9.4.3	Applications in nanomedicine	208
9.5	Conclusions and Future Outlook	210
10.	Bio-Applications of Functionalized Magnetic Nanoparticles and Their Nanocomposites	217
10.1	Introduction	217
10.2	Fundamentals of Nanomagnetism	220
10.2.1	Single-domain particles	220
10.2.2	Magnetic anisotropy energy	220
10.2.3	Superparamagnetism	221
10.3	Fundamentals of Colloidal Stability	223
10.4	Bio-Applications of Magnetic Nanoparticles	224
10.4.1	Magnetic separation	224
10.4.2	Drug delivery	225
10.4.3	Nuclear magnetic resonance imaging (MRI)	227

10.4.3.1	Contrast agents based on superparamagnetic nanomagnets.	228
10.4.4	Magnetobiosensors	231
10.4.4.1	Magnetobiosensors based on magnetorelaxometry	232
10.4.4.2	Magnetobiosensors based on magnetoresistance	233
10.4.4.3	Magnetosensors based on Hall effect	234
10.4.4.4	Magnetoplasmonics	234
10.4.5	Magnetic hyperthermia	235
10.5	Summary and Outlook	238
11.	Anti-Microbial Polymer Nanocomposites	249
11.1	Introduction	249
11.1.1	Packaging	250
11.1.2	Textiles	250
11.1.3	Coatings	252
11.1.3.1	Antimicrobial coatings	252
11.1.3.2	Medicine, pathology and surgical implants/ biomedical coatings	253
11.2	Anti-Microbial Polymer-Based Nanocomposites	253
11.3	Mechanisms of Antibacterial Action	256
11.3.1	Detection of microbes	256
11.3.2	Control of microbial growth	257
11.4	Environmental and Health Concerns	260
12.	Biosensing Applications Using Nanoparticles	265
12.1	Biosensors: A Definition	265
12.2	Uses of Gold Nanoparticles	266
12.2.1	Tailoring biointerfaces over gold nanoparticles	267
12.2.2	Biosensing applications of gold nanoparticles	268
12.2.2.1	Crosslinking-based biosensing	269
12.2.2.2	Non-crosslinking-based biosensing	272
12.3	Semiconductor Quantum Dots	273
12.3.1	Properties of quantum dots	273
12.3.2	Biosensing with quantum dots	273
12.3.2.1	Immunosensing	274
12.3.2.2	DNA assays	274
12.3.2.3	Resonance energy transfer-based assays	275
12.4	Outlook Remarks	277
	<i>Index</i>	283

List of Figures

1.1	Photograph of a polished ammonite and SEM image of a crystalline sediment in the fossil (bar = 5 μm).	3
1.2	SEM image of a fiber of a cellulosic nanocomposite (photograph on left bottom) containing silica-coated gold nanoparticles (TEM image on top right) (color Fig. C2).	6
1.3	Scheme of different nanoparticles surface modification methods.	7
1.4	Schematic representation of an energy diagram of a CdSe/ZnS core-shell nanostructure.	9
1.5	TEM of a core-shell particle composed of lanthanopolyoxometalates trapped in amorphous SiO_2 .	10
1.6	TEM images of poly(styrene)-based nanocomposite particles containing nano-fillers (dark areas) of EuS (left), ZnO:Er (center) and Au (right).	12
1.7	Examples of biomedical applications of nanocomposite particles.	13
2.1	Crosslinking reaction between gelatine and chitosan with epoxides.	22
2.2	Crosslinking reaction between gelatine or chitosan with genipin.	22
2.3	Scanning electron micrographs: (a) Toluene diisocyanate/polycaprolactone diol microparticles and (b) poly(3-hydroxybutyrate-co-3-hydroxyvalerate) microparticles.	23
2.4	Effect in drug concentration using different administration methods.	24
2.5	Chemical structures of alginate, chitosan and hyaluronic acid.	27
2.6	Chemical structures of inulin and dextran.	28
2.7	Transterification reaction catalyzed by Proleather enzyme.	29
2.8	Cyanoacrylates degradation in aqueous medium resulting in formaldehyde formation.	31
2.9	Formation of a urethane linkage.	32
2.10	Reaction between a pre-polymer and the amino groups of a protein resulting in a urea linkage.	32
2.11	Schematic representation of the chemical reactions involved in the PCL modified with 2-isocyanatoethylmethacrylate (IEMA) membrane synthesis (UV irradiation in the presence of Irgacure [®] 2959).	34

2.12	Scheme of a surface chemical grafting of a TPU using different chemicals and by previous functionalization with hexamethylene diisocyanate (HDI).	36
2.13	Scheme of surface grafting of a TPU with hydroxyethyl methacrylate (HEMA) using gamma irradiation.	36
2.14	Scheme of surface grafting of a TPU with hydroxyethyl methacrylate (HEMA) using UV irradiation and with isopropylthioxanthone (ITX).	37
2.15	Schematic representation of a plasma chamber	38
2.16	Schematic representation of plasma treatment effects.	39
3.1	Schematic diagram of nanocapsules containing an aqueous or oily core.	46
3.2	Preparation of nanocapsules by interfacial polymerization.	48
3.3	Preparation of nanocapsules by interfacial polymer deposition following solvent displacement.	49
3.4	Preparation of nanocapsules by polymer adsorption following solvent displacement.	50
3.5	Preparation of nanocapsules by phase inversion temperature.	51
3.6	Serum calcium levels in rats after oral administration of salmon calcitonin in an aqueous solution (sCT Sol) or encapsulated in chitosan nanocapsules (CS NC) at two different doses (250 and 500 IU/Kg), (mean \pm SE; $n = 6$).	53
3.7	Serum calcium levels in rats after nasal administration of salmon calcitonin (sCT, dose: 15 IU/kg) in aqueous solution (with or without CS) or encapsulated in the control nanoemulsion (NE) or in chitosan nanocapsules (CS NC); (mean \pm SE; $n = 6$). *Significantly different from salmon calcitonin solutions ($p < 0.05$). #Significantly different from nanoemulsion ($p < 0.05$).	55
3.8	Permeation of indomethacin through isolated rabbit cornea: (Δ) PCL nanoparticles, (\bigcirc) PCL nanocapsules, (\square) submicron emulsion, and (\bullet) commercial eye drops (Indocollyre [®]).	57
3.9	<i>In vivo</i> effects of paclitaxel-loaded lipid nanocapsules (LNC) treatment on the growth of F98 glioma cells implanted. (C, control; Px-LNC, paclitaxel-loaded LNC; Px, Taxol only; Px + PEG-HS, Taxol with Solutol HS15 solution).	59
3.10	Inhibition of Erwing sarcoma fusion oncogen (EWSFl11)-expressing tumor growth in nude mice by: \bigcirc , siRNA-antisense (siRNA-AS) loaded NC; Δ , siRNA-control loaded NC; \square , siRNA-AS naked; \diamond , siRNA-control naked; \bullet , saline.	60
4.1	Encapsulation of QD cores in silica (F = functional group).	73
4.2	Self-assembly of gold nanoparticle arrays using oligonucleotides.	79
4.3	A nanoplasmonic ruler for measuring nuclease activity and DNA fingerprinting.	80
4.4	Encapsulation of QDs in phospholipid micelles and conjugation with DNA by sulfo-SMCC.	81

4.5	A summary of the bioconjugation schemes. (A) Chemisorption of an electronegative group to positive ions on the nanoparticle surface, a thiolate linkage in this case. (B) A heterobifunctional crosslinker. (C) Conjugation by electrostatic attraction. (D) DNA intercalation. (E) Conjugation by affinity binding, antibody-antigen in this case. (F) Conjugation via a functionalized phospholipid.	82
4.6	(a) CdSe/ZnS QDs fluorescing from blue to red, with a diameter range of 2–10 nm. (b) A pseudocolor image of a human epithelial cell labeled with QDs. (Color Fig. C3)	85
4.7	Synthesis of QDs which self-illuminate by bioluminescence resonance energy transfer.	87
5.1	Detail of the surface of the <i>Thalassiosira sp.</i> frustule.	98
5.2	SEM image of a giant spicule.	100
5.3	Conversion of a diatom frustule from (a) silica to (b) MgO, followed by (c) BaTiO ₃ deposition. (d) shows corresponding XRD patterns.	101
5.4	Different silica morphologies obtained in the presence of the R5 peptide (scale bar = 1 μm).	104
5.5	Different silica morphologies obtained in the presence of poly-L-lysine (a-c, scale bar = 1 μm), together with selected electron diffraction pattern.	104
5.6	Silica microparticles formed by gelatin thin films templating.	106
5.7	Silica deposition on the surface of gelatine micro-beads.	108
5.8	Endocytosis and intracellular degradation of hybrid silica/biopolymer nanoparticles.	109
6.1	Nature example of a nanocomposite material: (a) shell with nacre surface; (b) mesolayers separated by organic layers embedded with CaCO ₃ ; (c) aragonite stacked platelets arranged in a ‘brick and mortar’ structure “glued” by a polymeric organic matrix. (Color Fig. C1)	116
6.2	Synthetic strategies to prepare polymer-based nanocomposite particles.	117
6.3	Examples of modified inorganic surfaces: <i>procedure 1</i> —adsorption of organic molecules; <i>procedure 2</i> —grafting of organic molecules through covalent bonds carrying: (a) reactive end groups; (b) polymerizable groups and (c) polymerization mediators.	119
6.4	Inorganic particles formed through sol-gel reactions in the presence of pre-formed polymers. The final nanocomposite can exhibit weak (a, b) or strong (c, d) interactions between the inorganic/organic components. The inorganic phase may consist in individual particles (a and c) or structured networks (b and d).	121
6.5	TEM images of SiO ₂ /poly(styrene) nanocomposites obtained with silica particles with (a) 72 and (b) 352 nm.	125
6.6	Scheme of the in situ emulsion polymerization in the presence of inorganic nanoparticles.	126

6.7	Schematic representation of the consecutive stages for the fabrication of the “Janus” nanoparticles.	126
6.8	Scheme of the in situ miniemulsion polymerization in the presence of inorganic nanoparticles.	127
6.9	Examples of ATRP initiators used in SIP ATRP from the surface of silica surfaces: (a) 2-(4-chloromethylphenyl)ethyl dimethylethoxysilane, (b) 3-(2-bromoisobutyryl)propyl di-methylethoxysilane and (c) 3-(2-bromopropionyloxy)propyl dimethylethoxysilane.	128
6.10	Examples of RAFT chain transfer agents used in RAFT SIP from inorganic surfaces: (a) 3-(2-Dithiobenzoatepropionyl)propyl dimethylmethoxysilane; (b) 4-cyanopentanoic acid dithiobenzoate and (c) 2-[[[(butylsulfanyl)carbonothioyl]sulfanyl propanoic acid].	130
6.11	Scheme for the different models of organization of the polymer chains grafted on inorganic nanoparticles: (a) compact-Au nucleus with polymeric chains (shell) completely folded; (b) extended-Au nucleus and polymeric chains (shell) completely extended radially, with all the chains in trans configuration and (c) height profile of a monolayer on a substrate.	131
6.12	Biofunctionalization of ferromagnetic latexes with bovine IG antibodies.	133
6.13	Targeting epidermal growth factor receptors (EGFR) with QDs. EGFR labeled with biotinylated epidermal growth factors (EGF), are stained with aminoQD covalently conjugated to streptavidin	134
7.1	Phase diagram of a single substance in the p,T space (S, Solid, L, Liquid, G, Gas, p, pressure, T, temperature, p_c , critical pressure and T_c , critical temperature).	147
7.2	Main routes towards metal-based NPs-polymer composites using SCFs.	151
7.3	New and versatile concept to form inorganic-organic hybrid NPs — Example of Pd NPs functionalized with heptadecafluoro-1-decanethiol.	153
7.4	Formation of inorganic NPs inside polymer particles. M-L is the metal precursor.	154
8.1	Magnetothermal responsive drug delivery using magnetic hydrogel composite nanoparticles; (a) nanocomposite particles containing magnetic nanoparticles and dispersed drug; (b) swelling/collapse of network gels caused by heat generated by exposing magnetic nanoparticles to an alternate external magnetic field; (c) drug release from network gel.	166
8.2	Effective (circles), Brown (solid lines) and Néel (dotted lines) relaxation times as a function of the nanoparticles diameter for two sets of K_{eff} and η values: $4 \times 10^4 \text{ J/m}^3$ $7 \times 10^{-4} \text{ Pa}\cdot\text{s}$ (typical values of magnetite in water) and $4 \times 10^5 \text{ J/m}^3$ $0.33 \text{ Pa}\cdot\text{s}$ (typical values of cobalt in glycerol). Other parameters are $T = 300 \text{ K}$ and $\tau_0 = 10^{-10} \text{ s}$	171
8.3	NMRD profile (R_1 as a function of ω_0) of magnetite nanoparticles in colloidal solution and fit to the outersphere model accounting for anisotropy. Insets show the relation between curve features and fit parameters.	173

8.4	(a) Transmission electron microscopy (TEM) image of FePt/Fe ₃ O ₄ core/shell nanoparticles; TEM (b) and HRTEM (c) images of FePt/Fe ₃ O ₄ heterodimeric nanoparticles.	178
8.5	Schematic representation of the hydrogel network of polysaccharides formed in the presence of cations: (a) G units “egg box” conformation in alginate and (b) κ -carrageenan helical conformation.	180
8.6	Average size of magnetite nanoparticles synthesized in the presence of κ -, ι - and λ - carrageenan, evaluated by XRD measurements.	181
8.7	TEM image of magnetic nanogels prepared in the presence of κ -carrageenan. The inner darker core indicates the presence of magnetic nanoparticles.	181
8.8	Scheme of the carbodiimide mediated reaction used for coupling the antibody to the surface of the magnetic carboxylated carrageenan nanospheres. Carbodiimide (EDAC) activates the carboxylic acid groups at the surface of the nanospheres to produce the reactive intermediate O-acylisourea which will react with amine groups in the antibody, giving an amide linkage.	182
8.9	TEM micrographs of Ni and Co nanoparticles prepared in the presence of alginate with low and high M/G ratio. (scale bar = 100 nm).	184
8.10	Schematic illustration of the LbL process to form polyelectrolyte multilayers on nanoparticles. Nanoparticles are consecutively coated using solutions of polyelectrolytes oppositely charged (1 and 2).	185
9.1	Schematic presentation of various types of magnetic-fluorescent nanocomposites.	195
9.2	Schematic presentation of general synthetic approach to fluorescently labeled silica coated magnetic nanocomposites. (i) Initial optional coating with sodium silicate; (ii) base catalyzed condensation of TEOS on nanoparticle surface; (iii) covalent attachment of carboxyl fluorophore to 3-aminopropyltriethoxysilane via EDC coupling step; (iv) condensation of silane-modified fluorophore onto silica coated magnetic particle.	197
9.3	Layer-by-layer treatment of magnetite nanoparticles with positively charged polyallylamine hydrochloride (PAH) and negatively charged poly sodium(styrene sulfonate) polyelectrolytes (PE).	199
9.4	Direct covalent linkage of magnetite nanoparticles to dopamine functionalized porphyrin.	202
9.5	Schematic presentation of the synthesis of FePt-CdS fluorescent magnetic nanocomposites.	202
9.6	Osteoblast cells uptake of particles. Population imaging (a) confocal image and (b) overlay with phase contrast (mag. $\times 40$, Scale bar = 50 μ m). Single cell imaging. (c) confocal image and (d) with combined phase contrast (mag. $\times 60$, Scale bar = 50 μ m). (Color Fig. C4)	205

9.7	Gross views of a rat brain labeled with TAT-conjugated QDs; (a) and (b) represent dorsal views and (c) represents coronal section. Pink color (left side in (a,c) and right side in (b)) originates primarily from QD fluorescence and background blue color (right side in (a,c) and left side in(b)) is due to the combination of UV excitation, autofluorescence, and scattering lights. (Color Fig. C5)	207
9.8	Leukocytes aligned between ferromagnetic lines. Whole blood was incubated with CD45-labeled ferromagnetic nanoparticles and acridine orange. (Color Fig. C6)	208
10.1	Comparison of the sizes of atoms, nanoparticles, and biological entities.	218
10.2	(A) Electron micrographs representing parts of the cytoplasm of HeLa cells after 1 h incubation at 37°C with magnetic nanoparticles ([Fe] = 10 mM) followed by 1 h chase. The nanoparticles (black points) are confined within endosomes, dispersed throughout the cell cytoplasm. (B) Electron micrographs of HeLa cells after 1 h incubation at 37°C with magnetic nanoparticles ([Fe] = 10 mM) followed by 1 h chase (including 30 min under a homogeneous magnetic field $B = 100$ mT). Chains of magnetic endosomes are observed along the magnetic field direction. (C) Living HeLa cell light transmission images. Chains of magnetic endosomes (pointed out with solid arrows) are oriented along the x direction of the magnetic field created by two pairs of Helmholtz coils.	219
10.3	A simple schematic representation of the superparamagnetic effect in absence of interparticle interactions. In absence of field all the moments points to the easy directions (single-domains are randomly oriented and the sum of magnetic moments is zero). After applying a high magnetic field all the moments orient parallel to that field and the magnetic moment reaches the highest value. After switching off the field two scenarios can be produced. In the scenario shown in the upper right part the thermal energy ($k_B T$) is not sufficient to overcome the anisotropy energy barrier (KV) and magnetic memory is developed. The magnetic moment sum equals to the so-called remanence magnetization (experimentally we observe the typical hysteresis loop associated with data recording). In the scenario shown in the lower right part the thermal energy ($k_B T$) overcomes the anisotropy energy barrier (KV) and as a result no magnetic memory is developed (superparamagnetic effect). The magnetic moment sum equals to zero as in the initial state (experimentally we observe reversibility, that is, no hysteresis). Important, these two scenarios are timely-dependent so using different techniques such as a vibrating sample magnetometer or Mössbauer spectroscopy (different measurements times) can lead to different results. In fact, any system is thermally relaxed to its initial conditions if it is left sufficient time without perturbation.	221

10.4	Release of 1-methyl-4-[2-(4-oxocyclohexadienylidene)ethylidene]-1,4-dihydropyridine (p-MOED) from loaded Fe_3O_4 @PCL hybrid particles in DMSO by magnetic heating.	226
10.5	Spin-echo abdomen magnetic resonance images of a living rat. Images in the first row were acquired before injection of the magnetic nanoparticles, and those from the second to the fourth row were captured at different times.	231
10.6	Schematic illustration of the synthesis and structure of the multifunctional magnetic gold nanocomposite (MGNC) for cancer detection via MRI and synchronous dual therapy.	232
10.7	Schematic of a scanning micro-Hall probe microscope including the electronic scheme of the experiment. Inset shows the scheme of the scribed Hall cross. The size of the Hall bar is in the range of 1–5 μm	235
10.8	The DNA-BCA assay. (A) Nanoparticle and magnetic microparticle containing nanomagnets probe preparation. (B) Nanoparticle-based PCR-less DNA amplification scheme.	236
11.1	Bacterial growth can be interfered in many ways. A schematic representation depicting the multiple modes of action of metal nanoparticles. A single type of particle can act on many components of bacterial cell growth.	258
11.2	Images showing the inhibition zones for samples of <i>E. coli</i> : (a) control, (b) with antibiotics, and (c) with synthesized Ag-PEG-PU- TiO_2 films. The images illustrate that the nanocomposite samples are more effective in creating a sharp zone of inhibition compared to the antibiotics. (Color Fig. C7)	259
12.1	Schematic example of biorecognition-induced aggregation of Au NPs. (a) Colloidal solution of probe-functionalized Au NPs and its typical optical absorption spectrum. (b) The biorecognition-induced aggregation of the functionalized Au NPs by means of interaction with the target analyte results in a plasmon peak shift towards higher wavelength as well as in broadening of the spectrum (solid line), which can be detected with the naked eye by a color change from red-to-blue of the colloidal solution.	268

12.2 Au NPs aggregation through interparticle crosslinking (left panel). (a) AuNPs are brought close together by target molecules having multiple binding sites for the receptors previously immobilized at the nanoparticles surfaces; (b) removal of crosslinking molecules promoting nanoparticle redispersion; (c) target modification of crosslinking molecules to avoid nanoparticle aggregation; and (d) target modification of the receptors to indirectly control aggregation and redispersion. AuNPs aggregation induced by direct recognition (right panel) of receptor-modified nanoparticles and complementary-modified nanoparticles: (e) Disruption of interparticle interaction to promote redispersion; (f) aggregation can be regulated by biological processes that modify surface-attached receptors. 270

12.3 Schematics of the strategy for the simultaneous detection of four different toxins. First, antibodies against all four toxins were adsorbed on a solid surface. Second, the immobilized antibodies were exposed to a mix of all four toxins. Third, toxins were detected by anti-toxin antibodies conjugated to the various QDs. 274

12.4 Schematics of the RET-based maltose-sensor with quantum dots as energy donors. 276

12.5 Conformational diagram of a molecular beacon in the presence and in the absence of the complementary target. 276

List of Tables

2.1	Monomers used in the synthesis of hydrogels.	26
2.2	Methods of surface modification techniques used in biomaterials.	35
3.1	Polymers used as wall materials in nanocapsules for the delivery of different therapeutics, using varied administration routes.	47
7.1	Critical coordinates of CO ₂ and H ₂ O.	147
8.1	Examples of natural polymers used in the preparation of hydrogels.	166
8.2	Examples of magnetic nanocomposite hydrogels.	178
11.1	Examples of nanocomposites exhibiting specific antimicrobial activity.	255

Preface

Over the past decades there has been a notable progress in the Science and Technology of Nanomaterials. The distinct and novel properties of nanostructured materials along with their size scale comparable to biological structures raised the interest of the pharmaceutical and biomedical industries in the field of Nanotechnology. As a result, a number of approaches has been developed aiming to produce high quality nanoparticles for several bio-applications. These efforts raise many issues related to the design of materials with specific functionalities and question how these materials interact with biological systems.

Although research on nanoparticles is evolving rapidly, nanocomposite particles have been less investigated particularly when biointerfaces are also considered in these studies. Analogous to single-phase nanoparticles, and besides chemical composition, size effects and surface structure are of great relevance in determining the properties of nanocomposite particles. However, because at least two distinct chemical components are present in such hybrid particles, there is the possibility of achieving new functionalities when compared to the individual components. Moreover, new effects can emerge due to specific physico-chemical interactions between the materials that compose the nanocomposites. This is a key feature with great consequences in many applications that to be fully developed need bridges between scientific domains that are frequently apart.

The main scope of this book is to introduce the reader to important aspects on the materials chemistry of nanocomposite particles and underpinning properties of relevance for various bio-applications. It is our aim to provide an overall picture of this field to readers, eventually having quite distinct scientific backgrounds, by covering the recent developments in nanocomposites particles. In this context, we have deliberately favored the presentation of topics of general interest to understand the properties of the materials in detriment of very specialized topics eventually circumscribed by a purist terminology.

While planning this book a number of relevant topics in nanocomposite science came to our discussions. We decided to maintain open slots covering the main aspects on nanocomposite particles for bio-applications and then to invite specialists to contribute for each envisaged topic. Chapter 1 is an introductory chapter to

general aspects on nanoparticles and their use as nano-fillers in nanocomposites. On the other hand, Chapters 2 and 3 are mainly concerned with the science of polymers normally used in nanocomposites, namely their chemical functionalization and their use in a biological context, such as in pharmaceutical and medical applications. In Chapters 4 and 5 there is a special focus on bionanocomposites and biointerfaces, bridging aspects presented previously in Chapters 1–3 to those that are dealt with in the subsequent chapters. Chapters 6–9 details synthetic routes towards diverse nanocomposite particles and also relevant properties aiming bio-applications. Finally, Chapters 10 to 12 offer examples of bio-applications that make use of nanocomposites and address a number of scientific challenges for their use in a biological context, including their health and environmental impact.

Nanotoxicological concerns are especially acute when considering bio-applications and in particular those with interest to Nanomedicine, because in this case all efforts are primarily directed to the well-being of the patient. These aspects are briefly mentioned in some of the chapters of this book. Nevertheless, nanotoxicology and nanosafety regulations are issues evolving rapidly to a specialized body of knowledge for scientists and regulatory agencies. Scientific literature concerning specifically nanotoxicology issues has been published and will be valuable for readers of this book.

The concept of this book was in a large extent inspired by a multi-disciplinary team involved in a project aiming to develop nanocomposite particles with potential for *in vitro* clinical diagnostic techniques (Project PTDC/QUI/67712/2006 funded by Fundação para a Ciência e Tecnologia/FEDER). To our colleagues and post-graduate students involved in this project we thank their long date collaboration.

We are pleased to have edited this book and we are very grateful to the authors of the chapters, for their essential contributions. This book would not be possible without their expertise and enthusiasm.

It is our hope that this book contributes not only for the state of the art on nanocomposite particles but also to convey a stronger impetus to research in this fascinating field. Nevertheless, we prefer to let the reader be the final judge of this contribution. Nanocomposite particles are small-scale materials promising a number of benefits but also a number of big challenges requiring a multi-disciplinary approach to tackle scientific issues and the engagement of diverse audiences. Somehow, this reminds us the inspired words of the poet Fernando Pessoa: "*All is worthwhile if the soul is not small*".

Aveiro, 2010

Tito Trindade
Ana Luísa Daniel da Silva